# The influence of longitudinal grooves on the performance of two-dimensional diffuser

A. M. El-Kersh

*Department of Mech. Power and Energy, El-Minia University, Egypt.*

Detailed measurements are carried out to investigate the effect of longitudinal small grooves on the performance and boundary layer characteristics of two-dimensional diffuser. A diffuser having 1.78 area ratio and 5.6 non-dimensional length is tested with smooth and grooved surfaces at inlet Reynolds number of $0.96 \times 10^5$, $1.19 \times 10^5$ and $1.41 \times 10^5$. Insignificant variation in static pressure recovery coefficient with Reynolds number is presented for smooth wall diffuser. The grooved surface diffuser showed an increase in static pressure recovery coefficients with increasing inlet Reynolds number due to reduction of exit blockage factor and velocity profile energy coefficient. However, these coefficients are deteriorated compared with those of smooth surface diffuser. Replacing the smooth surfaces with grooved ones leads to reduce the wall shear stress coefficient, whereas the shape factor and momentum thickness of boundary layers show the opposite effect. This influence is significant at lower values of non-dimensional groove depth, $h\, u_\tau / \nu$. The turbulent shear stress is reduced in the inner layer for the grooved surfaces particularly at lower inlet Reynolds number in which the peak of the shear stress moves slightly away from the wall. The non-dimensional entrainment is calculated from the boundary layer measurements and compared with empirical functions.

تم إجراء القياسات التفصيلية لبحث تأثير الحزوز الصغيرة الطولية على أداء الناشر الثنائى الأبعاد وعلى خصائص طبقته الجدارية، ولقد تم اختبار ناشر نسبة مساحة مقطع خروجه إلى دخوله هى ١,٧٨ وطوله اللابعدى هو ٥,٦ لحالتى الأسطح الملساء والمحززة عند أرقام رينولدز ٠,٩٦ x ١٠$^{٥}$، ١,١٩ x ١٠$^{٥}$ ، ١,٤١ x ١٠$^{٥}$ . ولقد وجد أن هناك تغيرا غير ملحوظ فى معاملات الضغط الإستاتيكى المسترد مع رقم رينولدز فى حالة الناشر ذو الأسطح الملساء ، ولقد أوضحت التجارب المعملية للناشر ذو الأسطح المحززة أن معاملات الضغط الإستاتيكى المسترد تزداد مع زيادة رقم رينولدز وذلك نتيجة لانخفاض عامل الانسداد عند الخروج ومعامل طاقة شكل السرعة ولكنها تتدهور مقارنة بحالة الأسطح الملساء، وعندما تم تغيير الأسطح الملساء بالأسطح المحززة أدى ذلك إلى تقليل معامل إجهاد القص عند الجدار بينما أدى ذلك إلى زيادة عامل الشكل وسُمك كمية التحرك للطبقة الجدارية، وهذا التأثير كان ظاهرا عند القيم الأصغر للارتفاع اللابعدى للحزوز، كذلك فإن إجهاد القص للسريان المضطرب للسطح المحزوز قد قل فى الطبقة الجدارية وخاصة عند القيم الصغرى لأرقام رينولدز والتى عندها نجد أن مكان القيمة القصوى لإجهاد القص قد تحرك قليلاً بعيدا عن الجدار، وأخيرا فأنه تم حساب انتقال السريان اللابعدى إلى الطبقة الجدارية من خلال قياسات الطبقة الجدارية ومقارنته ببعض الدوال التجريبية.

**Keywords:** Two-dimensional diffuser, Pressure recovery, Turbulent flow, Boundary layers.

## 1. Introductin

Diffusers are used in many internal flow systems to reduce the velocity level and hence increase the static pressure as the fluid moves from inlet to outlet. Numerous publications of diffusers with smooth surfaces are available to provide rough correlations of data, based on the experimental work, for performance prediction. In the case of straight-walled diffusers, charts are available for rectangular, conical and annular cross sections [1,2], which give rough assessment of diffusers pressure recovery for prescribed geometry. Recently, successful attempts have been presented to predict diffuser performance, including static pressure recovery, location of separation and stalled regions using different computational techniques [3,4].

In some internal flow systems, heat transfer plays a role as important as diffuser performance [5]. This in turn requires a compromise between diffuser performance and heat transfer requirements by selecting the proper area ratio and length of diffuser. The control of heat transfer in internal flow can be achieved by affecting flow structure near the wall by introducing artificial roughness of small ribs at regular intervals on the surface, which acts as mixing promoters. However, this technique increases the frictional losses and hence the pumping power [6]. Another efficient technique to enhance heat transfer without increasing pumping losses is presented; in which transverse triangular grooves are introduced [7]. A reduction in skin friction coefficient by about 6% at zero pressure gradient is demonstrated by several research workers resulting from covering the wall surface with small triangular riblets [8,9]. However this reduction is increased to 11% by introducing longitudinal microgrooves [10]. This discrepancy in the skin friction reduction may be attributed to the difference in the flow structure near the wall. In addition, in the adverse pressure gradient, increasing the pressure gradient leads to increase the reduction in friction coefficient up to 7% within the experimental range [11]. The measurements with a three-dimensional particle tracking velocimetry, for the channel flow along the riblet surface, showed that the drag reduction is associated with changes in inner region of boundary layers [12]. In addition, the streamwise vortex is modified by the riblets leading to attenuation in the production of turbulent energy.

Most of the above publications are limited to the flow behaviour along the riblet surfaces. Also few studies are presented for channel flow with riblet surfaces at zero pressure gradient. In the present work, tests have been carried out to assess the influence of longitudinal small triangular grooves on the flow structure and performance of two-dimensional diffuser.

## 2. Experimental apparatus

The layout of the experimental apparatus is shown in fig.1. Air enters the diffuser through two-dimensional intake of $w_i$ =100 mm and b= 200 mm cross section and 532 mm length which is equivalent to 4 inlet hydraulic diameter. A two-dimensional diffuser of an optimum geometry based on the performance chart of Reneau et al. [1] is selected. A diffuser area ratio of 1.78 and a which produce maximum pressure recovery for the selected non-dimensional length of $L/w_i$ = 5.6. The diffuser is tested with smooth and grooved surfaces. Longitudinal triangular grooves of 1.0 mm depth, 60 deg. apex angles and 3 mm pitches are processed on the divergent walls. The downstream end of the diffuser is connected to a two-dimensional duct followed with a plywood box, which acted as a settling chamber. The other end of the settling chamber is poltted directly to the suction side of a centrifugal blower, which draw the air through the rig. The blower is normally run at 2800 rpm with a power fan 2.2 kW and the air is finally exhausted to atmosphere.

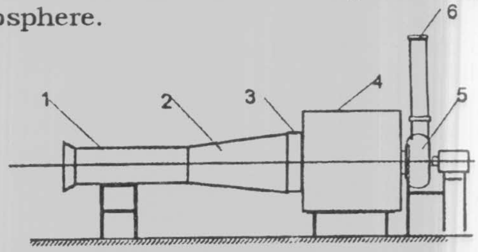


Fig. 1. Layout of experimental apparatus.

Velocity measurements are performed at several stations corresponding to the center plane of two diverging walls. Velocity measurements are taken by DISA constant temperature hot wire anemometer. The shear stress and turbulent intensity are measured as discussed in ref. [6]. Total pressure measurements are conducted by a total pressure tube of 0.6 mm diameter. Also the static pressure measurement is made at wall pressure taps using micro-manometer.
The calculated uncertainty in velocity, static pressure recovery and total pressure loss coefficients are 1.8%, 3.7% and 5.7% respectively.

## 3. Results and discussion

### 3.1. Performance of diffuser with smooth surfaces

The velocity profiles at five stations along the diffuser are shown in fig. 2. All velocities exhibit a uniform core and the maximum velocity decreases towards the diffuser exit resulting in a reduction of kinetic energy, which would be converted to the static pressure. The static pressure recovery and total pressure loss coefficients are defined respectively, by:

$$C_p = \frac{\bar{p}_e - \bar{p}_i}{\frac{1}{2}\alpha_i \rho \bar{u}_i^2} . \quad (1)$$

$$\lambda = \frac{\bar{P}_i - \bar{P}_e}{\frac{1}{2}\alpha_i \rho \bar{u}_i^2} . \quad (2)$$

From the energy equation across the diffuser, the relation between static pressure recovery and total pressure loss coefficient is given by:

$$C_p = [1 - \frac{\alpha_e}{\alpha_i}\frac{1}{AR^2}] - \lambda . \quad (3)$$

The first term in eq. (3) corresponds to a reduction of kinetic energy in the diffuser, which would be converted to the static pressure. On the other hand, the second term represents the total pressure loss coefficient of available energy occurring within the diffuser as a results of viscous effects. Total pressure loss coefficients of the diffuser are shown in table 1. They are weakly affected by the variations in inlet Reynolds number for the exit blockage factor, which is not affected, within the experimental error, by the variation of inlet Reynolds number as shown in table 2.

The local shear stress coefficient is calculated from the measured velocity profiles using the known Clauser technique, a typical plot of the results is shown in fig. 3. A significant logarithmic region near the wall is clear specially at initial stages of diffusion. However, the divergence from the linearity shown by the profiles towards the edge of the boundary layer indicates the large wake component associated with adverse pressure gradients. The boundary layer development along the diffuser wall as shown in fig. 4 demonstrates that the adverse pressure gradient causes the shape factor and

Table 1
Diffuser performance

| Diverging walls | $Re_i$ | $C_p$ | $\lambda$ |
|---|---|---|---|
| Smooth surfaces | $0.96 \times 10^5$ | 0.542 | 0.112 |
| | $1.19 \times 10^5$ | 0.545 | 0.114 |
| | $1.41 \times 10^5$ | 0.548 | 0.113 |
| Grooved surfaces | $0.96 \times 10^5$ | 0.498 | 0.082 |
| | $1.19 \times 10^5$ | 0.514 | 0.101 |
| | $1.41 \times 10^5$ | 0.528 | 0.109 |

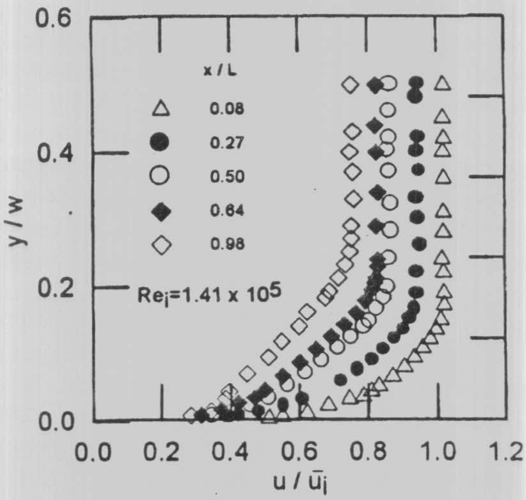


Fig. 2. Velocity profiles for smooth surface diffuser.

Table 2
Flow parameters at diffuser exit

| Diverging walls | $Re_i$ | $\alpha_e$ | $\beta_e$ |
|---|---|---|---|
| Smooth surfaces | $0.96 \times 10^5$ | 1.122 | 0.211 |
| | $1.19 \times 10^5$ | 1.109 | 0.207 |
| | $1.41 \times 10^5$ | 1.106 | 0.204 |
| Grooved surfaces | $0.96 \times 10^5$ | 1.363 | 0.274 |
| | $1.19 \times 10^5$ | 1.252 | 0.244 |
| | $1.41 \times 10^5$ | 1.184 | 0.218 |

momentum thickness to increase, whereas the wall shear stress coefficient has the opposite effect. The development turbulent shear stress along the wall of the diffuser is shown in fig. 5. The maximum shear stress increases as the flow proceeds downstream and moves away from the wall. This increase is more significant at the early stages of diffusion.

*3.2 Performance of diffuser with grooved surfaces*

The influence of grooved surface and inlet Reynolds number on the diffuser performance are summarized in table 1. In general the total pressure loss coefficient is slightly affected by increasing inlet Reynolds. However, significant increase in static pressure recovery is presented

At higher inlet Reynolds number. This enhancement is attributed to the reduction of exit blockage factor and velocity profile energy coefficient. The static pressure recovery is increased by 6% due to reduction of blockage factor at exit by 20% as the inlet Reynolds number increases from 0.96 x $10^5$ to 1.41 x $10^5$. Johnston [3] demonstrates that the rapid downstream growth of blocked area reduces the ability of the increasing physical area to diffuse the core zone and hence the recovery of the static pressure is reduced.

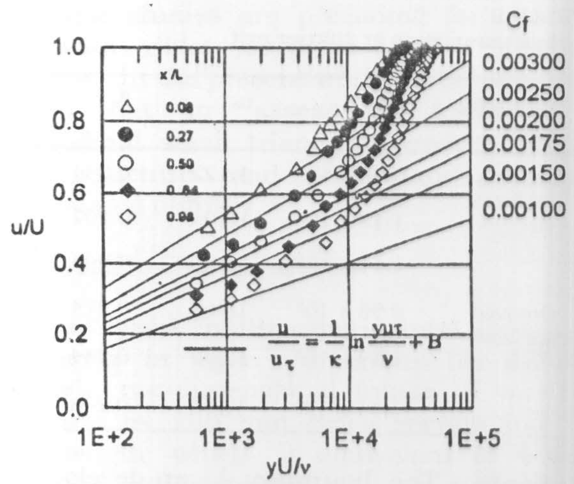


Fig. 3. Clauser plot of velocity profiles for smooh surace diffuser, $Re_i$ = 1.41 x $10^5$.

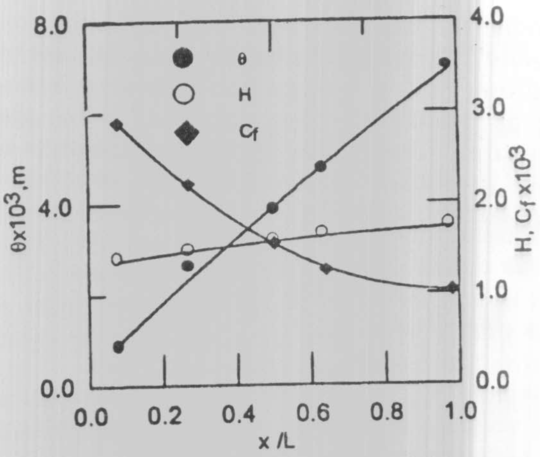


Fig. 4. Boundar layer development for smooth surface diffuser, $Re_i$ = 1.41 x $10^5$.

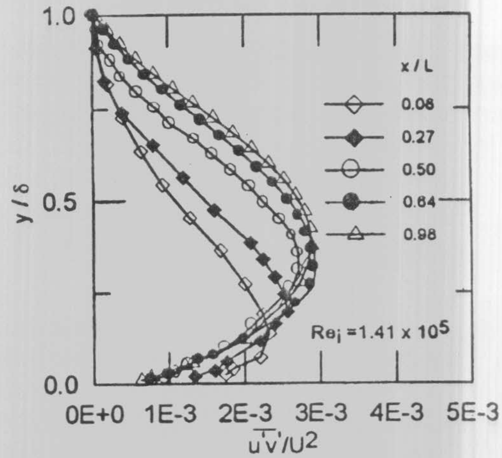


Fig. 5. Turbulent shear stress distribution for smooth surface diffuser.

A marked reduction in static pressure recovery is present when the diffuser smooth surfaces are replaced with grooved ones at the same inlet Reynolds number. This reduction is more pronounced at lower inlet Reynolds number. The static pressure recovery is reduced by 8.1% and 3.7% as the inlet Reynolds number is increased from 0.96 x $10^5$ to 1.41 x $10^5$. This is attributed to the increase of velocity profile energy coefficient and blockage factor at diffuser exit due to higher air entrainment from core to the boundary layer region as will be discussed at diffuser exit.

### 3.3. Structure of boundary layers

The above diffuser performance is associated with variations in boundary layer structure. The effect of grooved surfaces on the shear stress coefficient, shape factor and momentum thickness of the boundary layers compared with smooth surface diffuser are shown in Figs. 6-8. It is seen that, the ratio between the shear stress coefficient, shape factor and momentum thickness coefficient of grooved surface to that of smooth one can be correlated as function of non-dimensional groove depth ($hu_\tau/\nu$). Also, the results obtained along the diffuser for different inlet Reynolds number are overlapped and have the same trend.

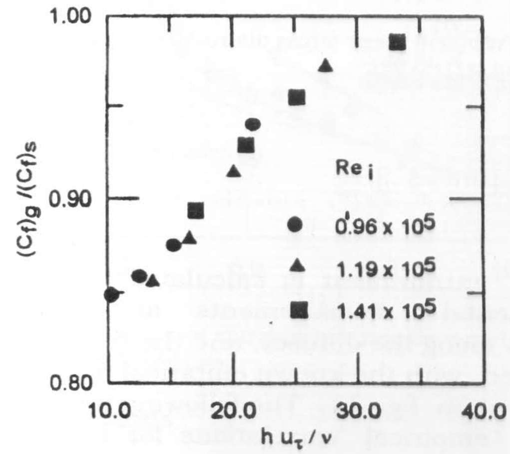


Fig. 6. Effect of grooves on the wall shear stress coefficient.

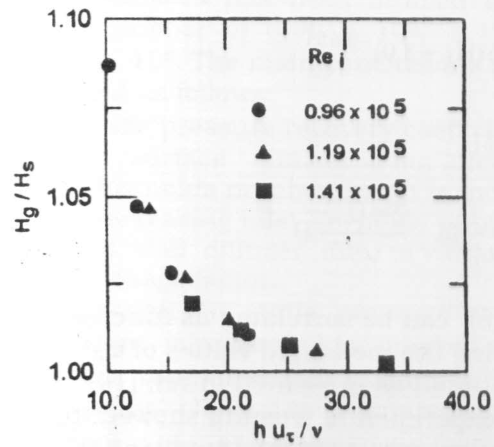


Fig. 7. Effect of grooves on the boundary layer shape factor.

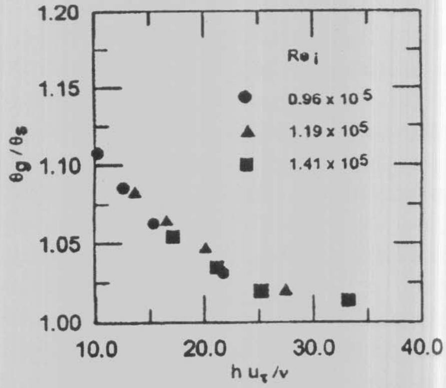


Fig. 8. Effect of grooves on the boundary layer momentum thickness

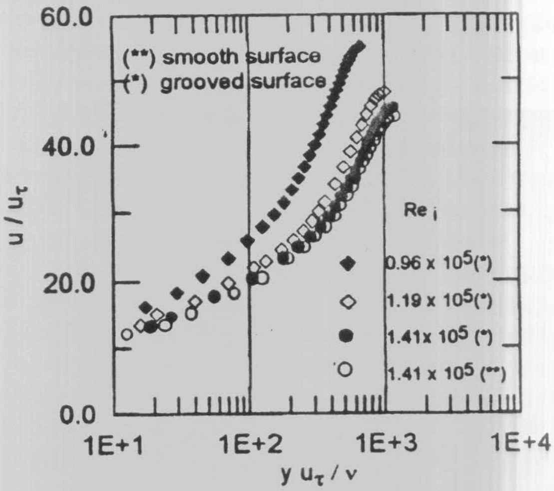


Fig. 9. Boundary layer velocity profiles near the diffuse exit (x/L=0.98).

Furthermore, replacing the smooth surface with grooved one in an adverse pressure gradient leads to reduce the wall shear stress coefficient, whereas the shape factor and momentum thickness have the opposite effect. It is noticed that a reduction in wall shear stress coefficient is obtained when the depth of grooves are less than the thickness of viscous sublayer and this is significant at lower values of ($hu_\tau/\nu$). Because the production of turbulent energy (i.e., the rate at which kinetic energy is transferred from the mean flow to the turbulence) is function of $u^3$, therefore its reduction for grooved surface compared with smooth surface diffuser is expected specially at lower values of ($hu_\tau/\nu$).

This is in agreement with the findings of Suzuki, Y. and Kasagi [12] for riblet surfaces. The maximum reduction in shear stress coefficient is about 15% at $(hu_\tau/\nu)=10$ and inlet Reynolds number of 0.96 x $10^5$. This is associated with an increase of the shape factor and momentum thickness of boundary layers by 8.7% and 10.6% respectively. In addition, the measurements with grooved surfaces showed a tendency in suppressing the turbulence level in the wall region. Increasing the shape and blockage factors at diffuser exit leads to reduce the static pressure recovery as shown in table 1. It is believed that, the effects of turbulence level and shape factors are interconnected as discussed by Klein [13], who demonstrates that the growth rate of the shape factors in a diffuser is retarded and hence performance improved irrespective of the turbulence level.

The boundary layer velocity profiles for smooth and grooved surafces at dissuser exit are shown in fig. 9. For the grooved surface, the velocity profiles are shifted upward compared with smooth surfaces at inlet Reynolds number equal to 1.41 x $10^5$. Furtherrmore, this shift of velocity is more pronounced for grooved surfaces as the inlet Reynolds number decreases. This is attributed to the reduction of wal shear stress coefficient.

The turbulent shear stress distribution across the boundary layer at diffuser exit is shown in fig. 10. The turbulent shear stress in the outer layer is the same for smooth and grooved surfaces and not affected by inlet Reynolds number. However, it is reduced in the inner layer for the grooved surfaces compared with smooth surfaces at inlet Reynolds number equal to 1.41 x $10^5$. The reduction in shear stress is more significant for grooved surfaces at lower inlet Reynolds number where the peak of the shear stress moves slightly away from the wall.

The prediction of diffuser performance by unified integral method depends mainly on the entrainment function [3]. It is an expression for the rate at which flow is transferred from the core into the boundary layers and defined by the following for two-dimensional boundary layers:

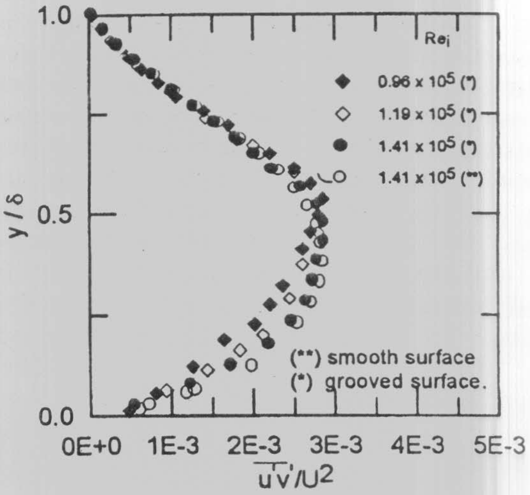


Fig. 10. Turbulent shear stress distribution near the diffuser exit (x/L=0.98).

$$E = \frac{1}{U}\frac{d}{dx}[U(\delta - \delta^*)] \quad (4)$$

The entrainment is calculated from the experimental measurements at different stations along the diffuser, and the results are compared with the known empirical functions as shown in fig. 11. The following functions present empirical correlations for the non-dimensional entrainment as established by Head and Escudier & Nicoll respectively [14]:

$$E = 0.0306(H_1 - 3.0)^{-0.653}, \quad (5)$$

$$E = 0.375\omega\Pi, \quad (6)$$

$$\Pi = \frac{\kappa}{2\omega} - \frac{1}{2}\ln\frac{\delta\omega U}{\nu} - B. \quad (7)$$

Eq. (6) can be correlated as function of $H_1$ by knowing the measured values of $\omega,\delta$ and U at each station as presented in ref. [14].

The experimental results showed that the entrainment increases by decreasing the form parameter $H_1$ downstream of the diffuser. The inspection of entrainment at each station of the diffuser showed that a significant increase is obtained with grooved surface diffuser by decreasing inlet Reynolds number. In addition, the experimental results are satisfactory with eq. (6), but eq. (5) shows significant differences at $H_1$ less than 6.5. This may be due to the dependence of the entrainment eq. (6) on the shear stress while eq. (5) is established for severe adverse pressure gradient, which is not the case of the present work.

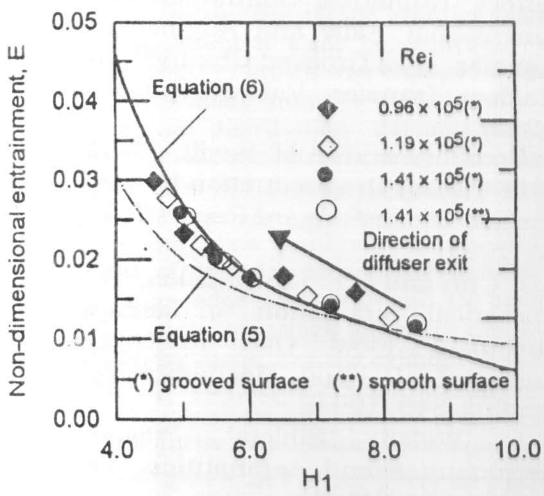


Fig. 11. Comparison of entrainmentr functions with the experimental results.

## 4. Conclusions

The performance of two-dimensional diffuser with smooth and small longitudinal grooved surfaces has been studied at inlet Reynolds number of $0.96 \times 10^5$, $1.19 \times 10^5$ and $1.41 \times 10^5$. The main conclusions may be summarized as follows:

1. The static pressure recovery coefficient of smooth surface diffuser is not affected by inlet Reynolds number, but it is increased with increasing inlet Reynolds number for grooved wall diffuser due to variations of exit blockage factor.
2. A reduction in static pressure recovery coefficient is presented for grooved surface diffuser compared with smooth diffuser at the same Reynolds number due to increase of exit blockage factor and velocity profile energy coefficient.
3. Replacing the smooth surface with grooved one leads to reduce the wall shear stress coefficient, whereas the shape factor and momentum thickness have the opposite effect considering that the depth of grooves ($h\ u_\tau\ /\nu < 30$) are less than the thickness of viscous sublayer.
4. The distribution of shear stress showed that its reduced in the inner layer for grooved surfaces particularly at lower inlet Reynolds number where the peak of the shear stress moves slightly away from the wall.
5. In an adverse pressure gradient, the entrainment has the tendency to increase with grooved surface compared with smooth one.

## Nomenclature

| | |
|---|---|
| A | cross sectional area |
| AR | diffuser area ratio, $A_e / A_i$ |
| b | diffuser breadth |
| | constant in velocity profile equation |
| $C_f$ | wall shear stress coeff., $\tau_w / \frac{1}{2}\rho U^2$ |
| $C_p$ | static pressure recovery coefficient |
| $D_h$ | hydraulic diameter at inlet |
| E | non-dimensional entrainment |
| h | height of the groove |
| H | boundary layer shape factor, $\delta^* / \theta$ |
| $H_1$ | form parameter, $(\delta - \delta^*) / \theta$ |
| L | diffuser axial length |
| p | static pressure |
| P | total pressure |
| Q | volume flow rate |
| Re | Reynolds number, $\bar{u} D_h / \nu$ |
| u | time average local axial velocity |
| $\bar{u}$ | mass derived mean velocity, Q / A |
| U | free stream velocity |
| $u_\tau$ | friction velocity, $\sqrt{\tau_w / \rho}$ |
| u' | fluctuating velocity component parallel to the wall |
| v' | fluctuating velocity component normal to the wall |
| x | distance along the wall |
| y | distance normal to the wall |
| w | distance between diverging walls |
| $\alpha$ | velocity profile energy coefficient, $\int_0^A (u/U)^3 dA / A$ |
| $\beta$ | blockage fraction, $2\delta^* / w$ |
| $\delta$ | boundary layer thickness |

$\delta^*$ displacement thickness, $\int_0^\delta (1-\frac{u}{U})dy$
$\theta$ boundary layer momentum thickness
$\kappa$ Von Karman constant
$\lambda$ total pressure loss coefficient
$\nu$ kinematic viscosity
$\rho$ fluid density
$\tau_w$ wall shear stress
$\omega$ wall shear stress parameter, $\sqrt{C_f/2}$

**subscripts**

e diffuser outlet
g grooved surface
i diffuser inlet
s smooth surface

**superscripts**

\- mean value

**References**

[1] L.R. Reneau, J.P. Johnston and S.J. Kline, "Performance and Design of Straight, Two-Dimensional Diffusers", ASME Journal of Basic Engineering, Vol. 89, pp. 141-150 (1967).

[2] G. Sovran and E.D. Klomp, "Experimentally Determined Optimum Geometries for Rectilinear Diffusers with Rectangular, Conical or Annular Cross Section", Fluid Mechanics of Internal Flow, G. Sovran, ed., Elsevier Publishing, New York, pp. 270-319 (1967).

[3] J.P. Johnston, "Review: Diffuser Design and Performance Analysis by a Unified Integral Method", ASME Journal of Fluids Engineering, Vol. 120, pp. 6-18 (1998).

[4] A.M. El-Kersh and K.Y. Khalil, "The Influence of Transverse Curvature on the Prediction of Flow Behaviour of An annular Diffuser", The First Minia International Conference For Advanced Trends in engineering, March 14-16, Vol. 4, pp. 1-12 (1999).

[5] S.Z. Shuja and M.A. Habib, "Fluid Flow and Heat Transfer Characteristics in axisymmetric Annular diffusers", Computers and Fluids, Vol. 25, pp. 133-150 (1996).

[6] A.M. El-Kersh, "Flow Pattern Past repeated Square Ribs In Rectangular Ducts", Bulletin of the Faculty of engineering, Assuit University, Vol. 27, No. 1, pp. 101-109 (1999).

[7] M. Greiner, G. Spencer and P. Fischer, "Direct Numerical Simulation of Three-dimensional Flow and Augmented Heat Transfer in a Grooved Channel", Journal of Heat Transfer, Vol. 20, pp. 717-723 (1998).

[8] E. Coustols and A.M. Savill, "Turbulent Skin-friction Drag reduction by active and Passive Means", Agard Report 786, pp. 8-80 (1992).

[9] D.C. Chu and G.E. Karniadakis, "A Direct Numerical Simulation of Laminar and Turbulent Flow Over Riblet-mounted Surfaces", J. Fluid Mechanics, Vol. 255, pp. 503-540 (1994).

[10] M.J. Walsh, "Riblets", Progress in Astronautics and Aeronautics, Vol. 123, pp.203-254 (1990).

[11] F.T.M. Nieuwstadt, W. Wolthers, H. Leijdens, K. Krishna and A. Schwartz, "The Reduction of Skin-friction by Riblets under Influence of Adverse Pressure Gradient", Exp. Fluids, Vol. 15 (1993).

[12] Y. Suzuki and N. Kasagi, "Turbulent Drag Reduction Mechanism Above a Riblet Surface", AIAA journal, Vol. 32, pp.1781-1790 (1994).

[13] A. Klein, "Review: Effects of inlet Conditions on Conical-Diffuser Performace", ASME Journal of Fluids Engineering, Vol. 103, p. 250-257 (1981).

[14] A.M. El-Kersh, "Investigations into Design and Performance of Annular Diffusers", Ph.D. Thesis, Paisley College of Technology, Scotland, (1983).

Received October 10, 2000
Accepted December 7, 2000